

# Numerical simulation of a fire resistance test and prediction of the flue gas leakage using CFD/FEM coupling

Fire resistance  
test and  
prediction of  
leakage

Rene Prieler and Simon Pletzer

*Institute of Thermal Engineering, Graz University of Technology, Graz, Austria*

Stefan Thusmer and Günther Schwabegger

*IBS–Institut für Brandschutztechnik und Sicherheitsforschung GmbH,  
Linz, Austria, and*

Christoph Hochenauer

*Institute of Thermal Engineering, Graz University of Technology, Graz, Austria*

Received 19 January 2023

Revised 15 March 2023

Accepted 27 March 2023

## Abstract

**Purpose** – In fire resistance tests (FRTs) of building materials, a crucial criterion to pass the test procedure is to avoid the leakage of the hot flue gases caused by gaps and cracks occurring due to the thermal exposure. The present study's aim is to calculate the deformation of a steel door, which is embedded within a wall made of bricks, and qualitatively determine the flue gas leakage.

**Design/methodology/approach** – A computational fluid dynamics/finite element method (CFD/FEM) coupling was introduced representing an intermediate approach between a one-way and a full two-way coupling methodology, leading to a simplified two-way coupling (STWC). In contrast to a full two-way-coupling, the heat transfer through the steel door was simulated based on a one-way approach. Subsequently, the predicted temperatures at the door from the one-way simulation were used in the following CFD/FEM simulation, where the fluid flow inside and outside the furnace as well as the deformation of the door were calculated simultaneously.

**Findings** – The simulation showed large gaps and flue gas leakage above the door lock and at the upper edge of the door, which was in close accordance to the experiment. Furthermore, it was found that STWC predicted similar deformations compared to the one-way coupling.

**Originality/value** – Since two-way coupling approaches for fluid/structure interaction in fire research are computationally demanding, the number of studies is low. Only a few are dealing with the flue gas exit from rooms due to destruction of solid components. Thus, the present study is the first two-way approach dealing with flue gas leakage due to gap formation.

**Keywords** Fire resistance test, CFD/FEM coupling, Deformation, Flue gas leakage

**Paper type** Research paper

## 1. Introduction

During fire resistance tests (FRTs), the thermal expansion (deformation) of a test specimen is a key issue for modern building materials exposed to a thermal load or fire, which is related to

---

© Rene Prieler, Simon Pletzer, Stefan Thusmer, Günther Schwabegger and Christoph Hochenauer. Published by Emerald Publishing Limited. This article is published under the Creative Commons Attribution (CC BY 4.0) licence. Anyone may reproduce, distribute, translate and create derivative works of this article (for both commercial and non-commercial purposes), subject to full attribution to the original publication and authors. The full terms of this licence may be seen at <http://creativecommons.org/licences/by/4.0/legalcode>

This work was financially supported by the Austrian Research Promotion Agency (FFG), “Virtuelle Bauteilprüfung mittels gekoppelter CFD/FEM-Brandsimulation” (Project 857075, eCall 6846234) and “Entwicklung von CFD/FEM Brandsimulationsmodellen mit Fokus auf Holz-und Gipsbauteile sowie komplexen Konstruktionen” (Project 876469, eCall 28585806).



---

the combustion and heat transfer in the gas phase (fire) and the thermal heat transfer in the solid test specimen. Standardized FRTs, according to [European Committee for Standardization CEN \(2012\)](#), using natural gas or oil-fired furnaces, with its pre-defined thermal load (time-dependent temperature trend), are carried out to determine the fire response (thermal resistance, mechanical stability and flue gas leakage from the furnace) of fire safety equipment. Based on the measured data, the test specimen can be certified for a certain fire resistance level. However, the FRTs are commonly related to high costs and time for the preparation, conduction and analysis of the tests. Thus, a logical consequence is to bring the FRTs, or at least some aspects, to the virtual space. Due to the increasing computational power, the simulation of FRTs has the potential to reduce extensive testing of test specimen before final certification for a certain fire resistance level.

### *1.1 Numerical modelling of FRTs*

A very popular approach applied in the past for modelling FRTs was the consideration of the gas phase combustion and thermal heat transfer in the solid test specimen by coupled computational fluid dynamics/finite element method (CFD/FEM) simulations [e.g. [Prasad and Baum, 2005](#); [Wickström et al., 2007](#); [Sandström et al., 2009](#); [Wickström et al., 2011](#); [Yu and Jeffers, 2013](#); [Cabova et al., 2017](#); [Lazaro et al., 2016](#)]. From the references above, it can be seen that numerical studies of fluid/structure interactions in fire science started around 2000 with an increasing number in the following years. The chemical reactions in the fire (flame) and the heat transfer in the gas phase are considered by CFD simulations based on the finite volume method. For this purpose, commonly commercial software packages like the fire dynamic simulator (FDS) ([McGrattan et al., 2013](#)) or ANSYS Fluent ([ANSYS, 2013](#)) are applied. The calculated heat fluxes from the gas phase to the solid test specimen were used for the thermal analysis using a FEM code. The heat fluxes from the CFD simulation are derived by the concept of the “adiabatic surface temperature” (AST) (see ([Wickström, 2016](#))), which is the temperature at the fire exposed surface of the test specimen. However, when gaseous components are released from the test specimen, the heat transfer as well as the combustion process can be affected and the AST results are doubtful [see ([Prieler et al., 2018a](#); [Prieler et al., 2019a](#))]. This can be the case for gypsum or wood parts, which release a significant amount of water vapour or combustible gases to the gas phase. [Prieler et al. \(2018a\)](#) proposed a methodology to address the conjugate heat transfer in solid gypsum and the gas phase in one CFD simulation without interface, leading to a better prediction of the gypsum’s temperature compared to the AST.

When the temperatures in the solids (test specimen) are known, the structural analysis caused by the thermal exposure can be done by coupled CFD/FEM simulations (e.g. ([Duthinh et al., 2008](#); [Alos-Moya et al., 2014](#); [Silva et al., 2014](#); [Silva et al., 2016](#); [Malendowski and Glema, 2017](#); [Szymkuć et al., 2018](#))). These simulations can be denoted as one-way coupling (weak coupling) according to the definition in [Welch et al. \(2008\)](#) and [Tondini et al. \(2012\)](#). This means that the deformation process does not affect the heat transfer or the gas phase (fluid flow and heat transfer). Thus, no flue gas leakage can be predicted.

In FRTs, as well as real fire scenarios, gaps between the solids and cracks/failures of components can lead to a flue gas leakage or a different ventilation situation of the fire. So, the deformation/thermal stresses can affect the combustion processes and heat transfer, which increases the complexity of the numerical modelling. Recently, first approaches were published [see ([Feenstra et al., 2018](#); [de Boer et al., 2019](#))], considering an office room fire and the failure of the façade elements, which reveals an additional exit for the flue gas to the ambient side. The mentioned studies above considered the flue gas leakage due to the mechanical failure of the solid components. However, flue gas leakage can also be observed between solid parts, which separate from each other due to the deformation. This was

---

addressed by [Prieler \*et al.\* \(2019b\)](#), where a fire exposed three-parted steel door was investigated by coupled CFD/FEM simulation. Although the simulation approach was only a one-way coupling, the gap formation was modelled and potential flue gas leakage was estimated and compared to the observations during the FRT. The position of the flue gas leakage was well predicted.

### *1.2 Objectives of the present study*

Since it was shown that studies considering the effect of mechanical failure or gap formation between the solid components on the combustion process and flue gas leakage are rare, the present study introduces a simplified two-way coupling approach (STWC) for the simulation of FRTs. The STWC is an intermediate approach between the one-way and two-way approach and will be used for a FRT of a fire safety steel door, which is embedded within a wall made of bricks. When using the STWC, the heat transfer within the steel door was calculated by a simple one-way approach, and the predicted temperatures are used in the two-way simulation, which means that the heat transfer in the solid was decoupled from the two-way methodology. Due to the STWC, the gap formation during the FRT as well as the deformation process of the steel door will be predicted. Thus, the present study considers the following objectives:

- (1) FRT of a fire safety steel door determining the temperatures within the door and its deformation
- (2) Prediction of the gas phase combustion and heat transfer within the test specimen (steel door) during the FRT with a one-way coupling methodology
- (3) Numerical analysis of the deformation of the steel door using the one-way coupling approach and the proposed STWC
- (4) Calculation of the gap formation and flue gas leakage during the FRT using the STWC

It has to be mentioned that only the door was considered in the structural analysis (deformation process), and the mechanical response of the adjacent wall was neglected. However, the mechanical behaviour of the brick wall has a significant effect on the deformation of the door and vice versa. This was investigated in detail in [Prieler \*et al.\* \(2019b, 2022a\)](#). Thus, modelling of the adjacent brick wall should be taken into account for future studies of FRTs. A first approach can be found in [Prieler \*et al.\* \(2022b\)](#).

## **2. Experimental setup**

### *2.1 Fire resistance testing furnace, wall and steel door*

For the validation of the predicted door temperature, deformation, gap formation and flue gas leakage, an FRT with a fire safety steel door as test specimen was done according to the standard ([European Committee for Standardization CEN, 2012](#)). The tested steel door was embedded into a wall made of bricks, which was placed at the front of a fire resistance testing furnace. This is illustrated in [Figure 1](#). The furnace dimension was  $4 \times 4.5 \times 1.25$  m. According to the standard, the furnace was heated up based on a pre-defined temperature trend, which enables a similar thermal load on the test specimen in each FRT. To achieve the pre-defined temperature, the furnace was operated by four natural gas burners at the side walls. For a more homogeneous temperature distribution in the furnace, baffle sheets were placed at each burner to deflect the flame [see ([Prieler \*et al.\*, 2018b](#))]. The temperature inside the furnace was observed using 12 plate thermocouples. These thermocouples were placed in a distance of about 10 cm from the fire exposed surface of the wall/door. The bricks had a thickness of 17 cm, and mortar was placed between the row of bricks.



**Figure 1.**  
Fire resistance test furnace (left) and wall made of bricks with embedded steel door (right)

**Source(s):** Author's own creation

In the centre of the wall the test specimen (fire safety steel door) was placed, with its thickness of  $64\text{ mm}$ . Basically, the door was made of a steel enclosure (thickness of  $1\text{ mm}$ ). The steel enclosure was filled with mineral wool and a gypsum plasterboard (thickness of  $6\text{ mm}$ ) in the middle of the cross-section, which increases the thermal resistance. Furthermore, the building dimension of the door was  $1.375\text{ m}$  (width) and  $2.5\text{ m}$  (height). The door's frame was fixed at the wall at 11 positions [see (Prieler *et al.*, 2022b)]. In addition, the door leaf was also connected with the frame by two hinges, the door lock as well as three security bolts. The positions of the connections between the door and the frame are shown in Figure 2 (left). To determine the temperature of the door, several thermocouples were placed at the fire unexposed side of the door. For validation, only 6 data points were used, which represent the average and maximum temperatures at the door (see Figure 2 (left)). The measurement positions "P1" and "P6" were placed in a distance of  $25\text{ mm}$  from the doors edge/corner. Here, the highest temperatures occurred during the FRT due to the higher thermal conductivity of the steel shell compared the mineral wool/gypsum board (thermal bridge). Furthermore, "P2", "P4" and "P5" were arranged in a distance of  $100\text{ mm}$ , and "P3" was located at the door's centre. The deformation was optically measured by a camera system during the FRT. For this purpose, marker spots were fixed at the door in accordance to the black dots in Figure 2 (right).

The duration of the FRT was 40 min, and the simulation using one-way coupling was carried out for this time frame. Since the highest deformation and flue gas leakage was already reached after several minutes, only 10 min of the testing time were considered in this study for the STWC. This was done because the calculation time using the STWC was much higher compared to the one-way coupling. Thus, considering only the first 10 min of the FRT was reducing the calculation time when the STWC was used.

## 2.2 Material properties

For the thermal and structural analysis of the test specimen (steel door), the temperature-dependent material properties of steel, mineral wool and gypsum are necessary.

Fire resistance test and prediction of leakage

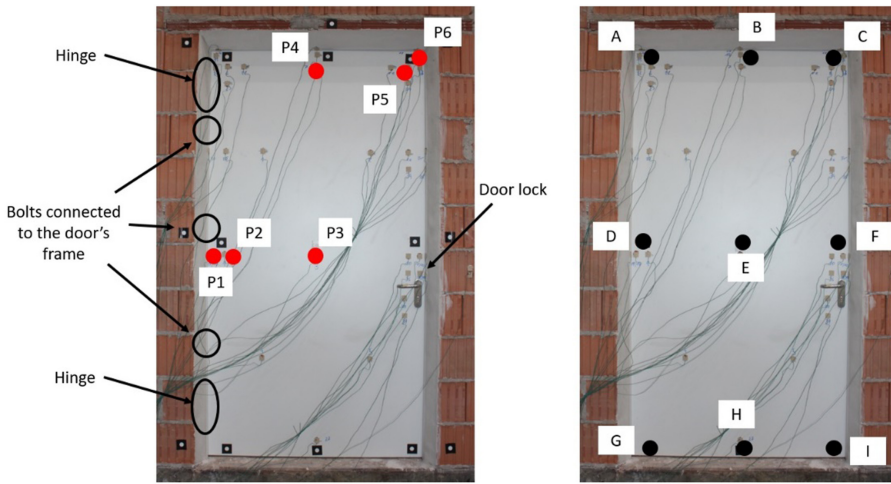


**Figure 2.** Connections between the door and the frame as well as temperature measurement positions (left) and position of the deformation measurement (right)

Source(s): Author's own creation

The thermal properties for low-alloy steel were calculated using the software JMatPro (JMatPro, 2005). In Figure 3 the temperature-dependent thermal conductivity and specific heat capacity are shown (see Prieler et al., 2016), whereas the density was set to a constant value of  $7,850 \text{ kg/m}^3$ .

The thermal expansion coefficient for steel and elastic modulus are presented in Table 1, where the values for the thermal expansion and Poisson ratio were chosen from (Richter, n.d.) and the elastic modulus as well as the multi-linear hardening in Figure 4 was derived from Luecke et al. (2011) with coefficients from Zhang et al. (2016). The model of Luecke et al. (2011) was used in this study to predict the stress-strain behaviour at high temperature, because Luecke et al. determined that it predicts the stress-strain behaviour slightly better than the Eurocode three (BS EN1993-1-2, 1993).

Gypsum, which was used inside the door, mainly consists of calcium sulphate di-hydrate ( $\text{CaSO}_4 \cdot 2\text{H}_2\text{O}$ ). During the heating phase, chemically bound water from gypsum is released by two endothermic reactions. These reactions can be identified by two peaks in the

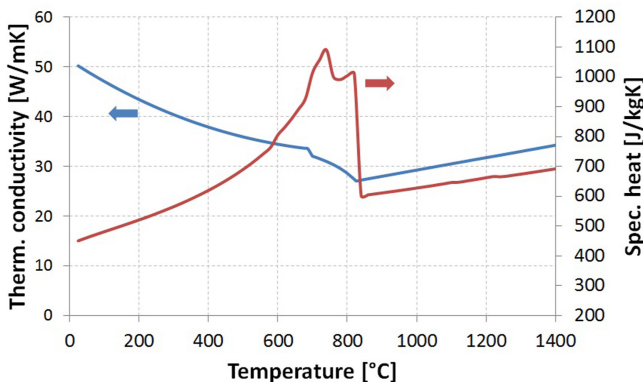


**Figure 3.** Thermal conductivity and specific heat capacity for low-alloy steel

Source(s): Prieler et al. (2016)

**Table 1.**  
Thermal expansion,  
Poisson ratio (Richter,  
n.d.) and elastic  
modulus (Luecke *et al.*,  
2011; Zhang *et al.*, 2016)

Temperature [°C]	Therm. Expansion coefficient (*10 <sup>-6</sup> 1/K)	Poisson ratio (F02D)	Elastic modulus (MPa)
20	11.9	0.282	215,000
50	12.1	0.286	213,053
100	12.5	0.287	209,809
150	12.8	0.288	206,439
200	13.0	0.290	202,729
250	13.3	0.291	198,404
300	13.6	0.293	193,150
350	13.8	0.295	186,640
400	14.1	0.297	178,563
450	14.3	0.299	168,669
500	14.5	0.302	156,814
550	14.7	0.306	143,009
600	14.9	0.311	127,459

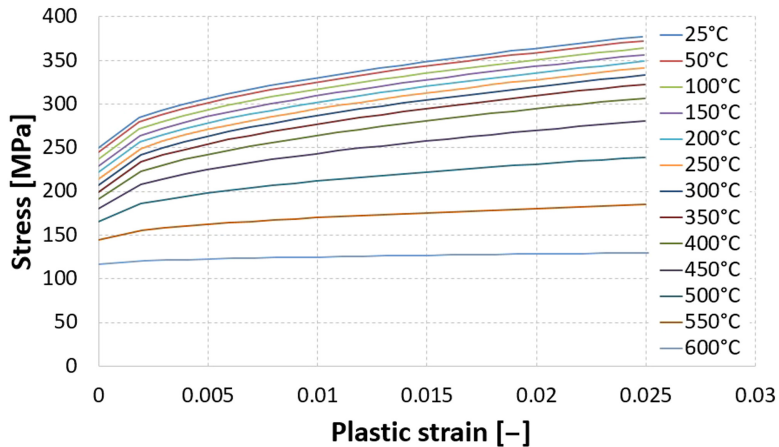


**Figure 4.**  
Calculated stress–  
strain curve of steel

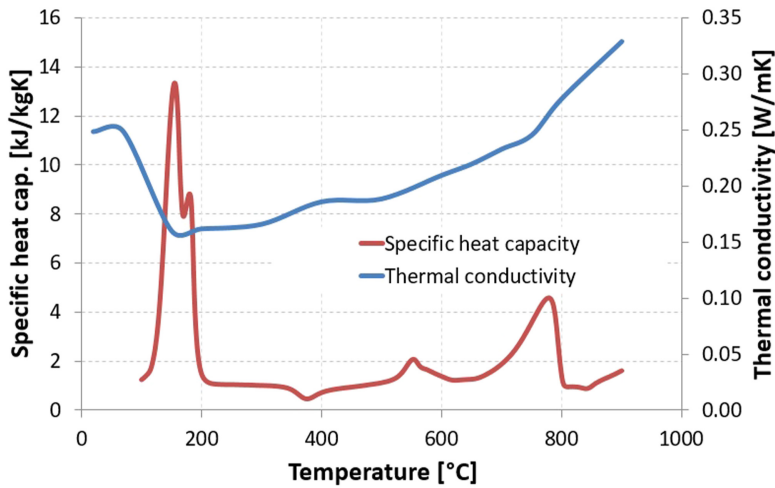
Source(s): Figure from Prieler *et al.* (2019b)

temperature-dependent specific heat capacity (see Figure 5). In Figure 5, the thermal conductivity of gypsum is shown. The density of gypsum was  $1,012 \text{ kg/m}^3$ .

The thermal properties of the mineral wool in the simulation were set in accordance to the manufacturer's data sheet with a density of  $185 \text{ kg/m}^3$  and a specific heat capacity of  $1,030 \text{ J/kgK}$ . In contrast to the constant values above, the thermal conductivity was considered as temperature-dependent as presented in Figure 6.

Since steel shows the highest thermal expansion and mineral wool/gypsum have minor mechanical stability compared to steel, only the steel enclosure of the door was considered in the structural analysis. Thus, no mechanical properties were used for mineral wool and gypsum.

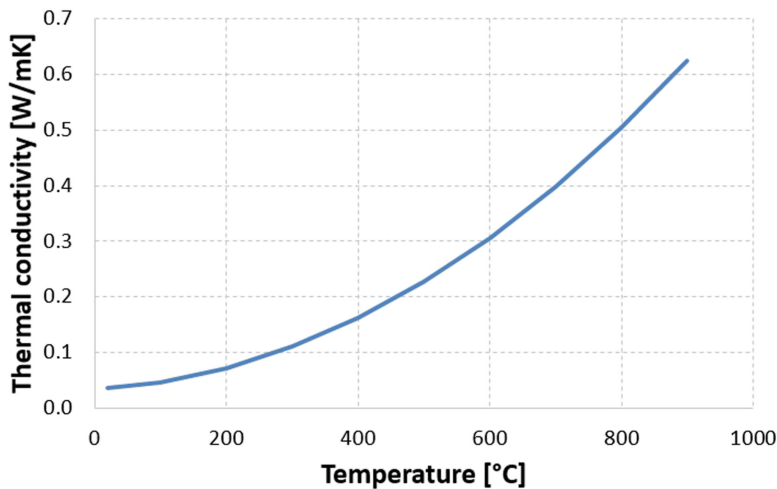
For the simulation of the gas phase combustion and the conjugate heat transfer in the test specimen, the heat transfer in the adjacent wall has to be taken into account. The thermal properties were defined by constant values for specific heat capacity and thermal conductivity with values of  $950 \text{ J/kgK}$  and  $0.425 \text{ W/mK}$ , respectively. The density was set to  $850 \text{ kg/m}^3$ .



Source(s): Prieler *et al.* (2020)

Fire resistance  
test and  
prediction of  
leakage

**Figure 5.**  
Temperature-  
dependent specific heat  
capacity and thermal  
conductivity of  
gypsum



Source(s): Author's own creation

**Figure 6.**  
Temperature-  
dependent thermal  
conductivity of  
mineral wool

### 3. Numerical methodology

Two approaches were used to numerically predict the fire response of the fire safety door: (1) one-way coupling and (2) a STWC of the CFD/FEM simulation. For this purpose, the commercial software package ANSYS 2020 R2 was used with its sub-packages ANSYS Fluent to predict the fluid flow (CFD) and ANSYS Mechanical for the structural analysis (FEM). Detailed information on the sub-packages, including transport equations to be solved, etc. can be found in [ANSYS \(2020a, b\)](#).

### 3.1 One-way coupling

In this one-way coupling approach, the gas phase combustion in the furnace and the heat transfer in the solid test specimen and adjacent brick wall were considered in one CFD simulation. The calculated temperatures in the solids from the CFD simulation were further used for the structural analysis of the steel door. In contrast to other one-way coupling approaches mentioned in section 1.1, no FEM code was used to predict the heat transfer in the solids. This would allow also the consideration of gaseous components released from the solids (e.g. water vapour from gypsum or combustible gases from wood), however this is not necessary in this study. Furthermore, it has to be mentioned that the adjacent brick wall was considered as rigid body without deformation. The calculated temperatures (local and temporal) in the solid test specimen were transported to the FEM code, where the structural analysis was carried out. The methodology of the one-way coupling approach is shown in Figure 7 and is completely described in Prieler *et al.* (2019a, b), where also the validation of the used commercial software package for the one-way coupling is presented.

Since the numerical grid for the CFD and FEM simulation are not identical with regard to the test specimen, the calculated temperatures from the CFD simulation have to be mapped on the numerical grid for the structural analysis. For this purpose, a “profile preserved” mapping methodology, which is presented in Figure 8, was used. In Figure 8, the temperatures in the CFD simulations are calculated at the positions of the red dots. However, before they can be used in the FEM simulation, they have to be mapped on the positions  $\alpha_i$ . In the present one-way approach, the closest nodes to  $\alpha_i$  were used to create a virtual tetrahedron around  $\alpha_i$ . Depending of the position of  $\alpha_i$  within the tetrahedron, weighing factors can be derived and the temperature at  $\alpha_i$  can be determined.

**3.1.1 Numerical grid and boundary conditions.** The numerical grid of the furnace was created by using 3.7 million polyhedrons (gas phase + walls + test specimen) and is presented in Figure 9. The natural gas input to each burner was 147 kW during the testing time of 40 min. In addition, the air mass flow-rate to the burners was adapted to ensure that the residual oxygen concentration in the flue gas was 6 vol%. Thus, the mass flow-rate of natural gas (considered as methane in the simulation) and air were used as boundary condition for the one-way coupling. The boundary condition at the outer surfaces of the simulation domain (walls and test specimen) was defined by convective (heat transfer coefficient: 4 W/m<sup>2</sup>K) and radiative heat losses (emissivity: 0.5) to the ambient side (ambient

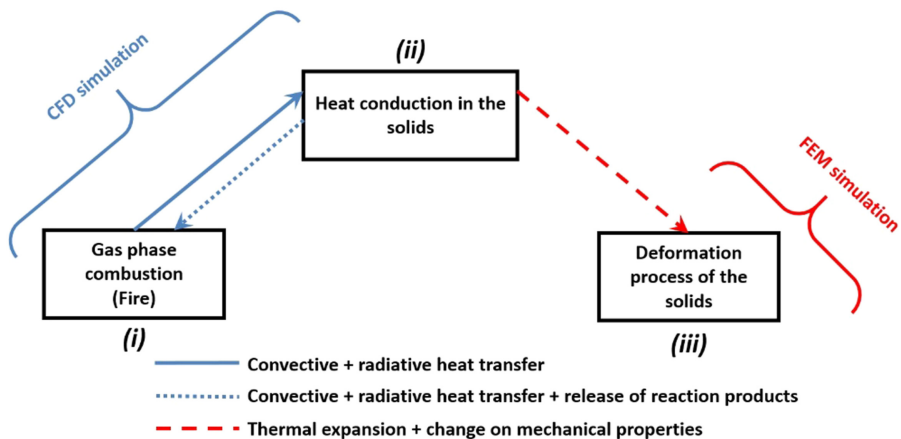
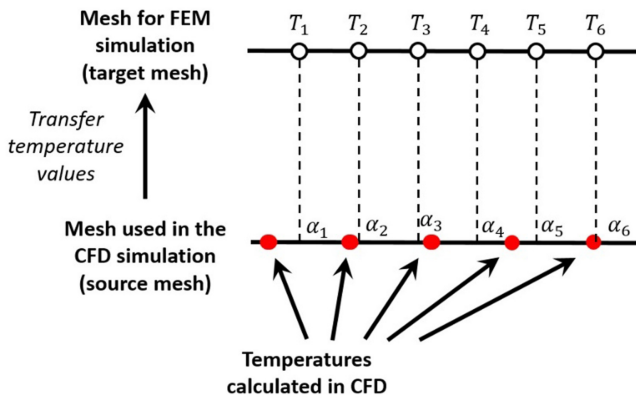


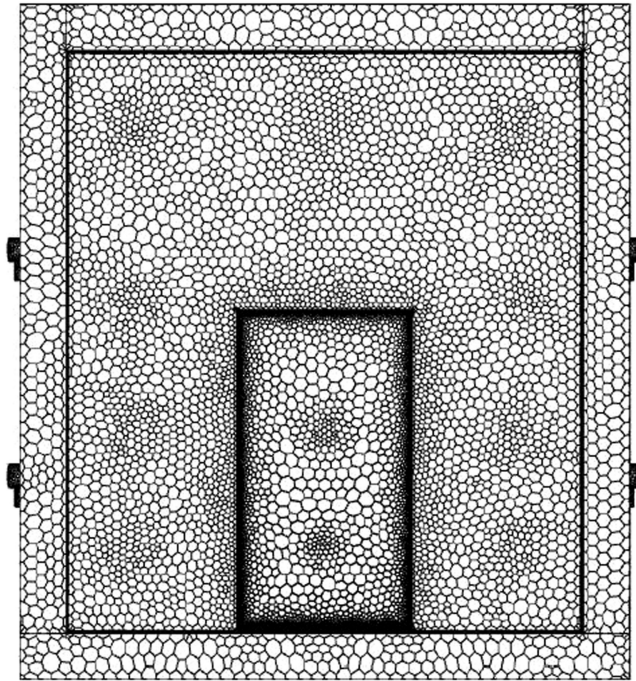
**Figure 7.** Methodology for the one-way coupling approach

Source(s): Author's own creation



Source(s): Figure from Prieler *et al.* (2019b)

**Figure 8.** Mapping methodology to transfer the temperature value from CFD (source) to FEM (target)



Source(s): Author's own creation

**Figure 9.** Numerical grid of the furnace for the CFD simulation using the one-way coupling

temperature: 25°C). The time step size was fixed with values of 1 s (0–120 s), 2 s (120–240 s) and 5 s (240–2,400 s).

For the structural analysis in the FEM simulation, the steel shell of the door as well as the door's frame were modelled by 69.000 tetrahedron cells. It was assumed that the adjacent wall was a rigid body, therefore also the door's frame, which was fixed with the wall, was assumed

---

to be rigid. The door was connected with the frame in the structural model by fixed connections using the multi-point constraint (MPC) formulation. These connections match with the position of the security bolts, hinges and the door lock (see [Figure 2](#)). In this formulation, the nodes from the frame and the door are sticking together during the entire testing time. The other faces of the door can get in contact with the frame (collide) due to the thermal expansion. However, although they get in contact, a relative (frictional) movement is possible. To describe this behaviour an augmented Lagrange formulation between the door and the door's frame was defined. For a better numerical stability, a small penetration was allowed for these faces, and the stiffness factor was set to a value of 0.1. Further details can be found in [Prieler \*et al.\* \(2019b\)](#). It has to be mentioned that water vapour from the gypsum board inside the door is released during the heating process, which increases the pressure inside the door. This was compensated by a linear pressure increase inside the steel shell from 0 to 0.15 bar between 0 and 1,200 s testing time. This was already suggested in the work of [Prieler \*et al.\* \(2021\)](#).

*3.1.2 Combustion and radiation modelling.* To predict the gas phase combustion, the Reynolds-averaged Navier–Stokes equations were solved in the CFD simulation using the realizable k-epsilon model proposed in [Shih \*et al.\* \(1995\)](#). The chemical reactions in the flames were calculated by the so-called steady laminar flamelet model (SFM) for non-premixed combustion. In this approach, proposed by Peters [see ([Peters, 1984, 1988](#))], the flame front of a turbulent flame can be approximated by a number of small laminar counter-flow diffusion flamelets. The main advantage of this assumption is that in a laminar counter-flow diffusion flamelet the thermo-chemical state at each position in the flamelet (flame front in turbulent flames) can be described by a single parameter called the mixture fraction  $f$ . Thus, the temperature, species concentrations and density of the gas are related to a single parameter, and this relation can be pre-calculated and stored in look-up tables. Subsequently, the chemistry calculation and solving the species transport equations during the CFD simulation can be avoided. There are only two transport equation for the mixture fraction and its variance to be solved, which couples the thermo-chemical state with the turbulent flow field via a probability density function.

The discrete ordinates model (DOM) [see ([Raithby and Chui, 1990; Chui and Raithby, 1993](#))] was used to solve the radiative transfer equation (RTE) for each discrete angle/direction. In the present study, a number of 128 directions for the radiative heat transfer were considered leading to the same number of RTEs to be calculated. Scattering effects were neglected in the furnace and the absorption coefficient of the flue gas in the furnace was predicted by the weighted sum of grey gases model (WSGGM) with coefficients by [Smith \*et al.\* \(1982\)](#).

### *3.2 Simplified two-way coupling (STWC)*

The numerical approach, denoted as STWC, represents an intermediate method between the one-way and the full two-way coupling (consideration of all processes and interactions in the simulation). A full two-way coupling was not reasonable because of two issues regarding the heat transfer in the solid test specimen and the large dimension of the testing furnace:

- (1) The heat transfer through the steel door and the deformation was not simulated simultaneously, caused by the missing knowledge about the contact between the mineral wool and gypsum board inside the door as well as the steel enclosure during the deformation. The deformation and contacts are very important for the heat transfer in the door, however, due to the deformation, the contact faces between mineral wool, gypsum board and steel can separate from each other. Subsequently, a continuous heat conduction through the solids can be highly affected. Due to the separation of the contact faces in the simulation, also numerical instabilities were detected in a pre-study.

- (2) Since the dimension of the testing furnace is large ( $4.5 \times 4 \times 1.25$  m), the calculation time would increase significantly for a full two-way approach. Therefore, the domain around the burners was neglected and the velocities, gas temperature, radiation intensity and pressure were extracted from the one-way simulation of the furnace for each time step. Thus, the transport equations for the reaction chemistry in the flame (fire) can be neglected in this STWC approach using a reduced domain, which saves calculation time.

Based on these issues, a full two-way coupling was not carried out and a simplified approach was introduced in this study, which is shown in Figure 10. It can be seen that the heat transfer in the solid test specimen was excluded in the STWC methodology. Therefore, the temperature data of the steel door from each time step were used from the one-way coupling simulation (see section 3.1). The mapping methodology, which brings the temperatures from the numerical grid of the CFD simulation to the FEM simulation, was also the same. Nevertheless, the fluid flow and heat transfer in the fluid was fully coupled with the deformation of the steel door, leading to the prediction of the gap formation as well as the flue gas leakage from the furnace to the ambient side.

As mentioned above, a reduced domain of the fluid flow was considered to save computational time. In Figure 11 the geometry of the simulation domain using the one-way-coupling approach is presented. Furthermore, the part of the gas phase in the furnace, which is considered in the STWC, is marked in blue. It can be seen that this region covers the vicinity of the test specimen (steel door).

To predict the flue gas leakage in the STWC methodology, the gas phase at the ambient side has to be considered in the simulation too. The region at ambient side is highlighted by the red marked zone in Figure 12 (left). In this figure, the blue zone represents the gas phase inside the furnace. The red and blue zone in Figure 12 (left) stands for the entire gas phase in the simulation using STWC. The boundary at the ambient side was defined as pressure-outlet with a defined pressure of 1,013, 25 mbar. If backflows in the simulation domain occur, the incoming fluid was defined as air with a temperature of 25°C. At the boundary inside the

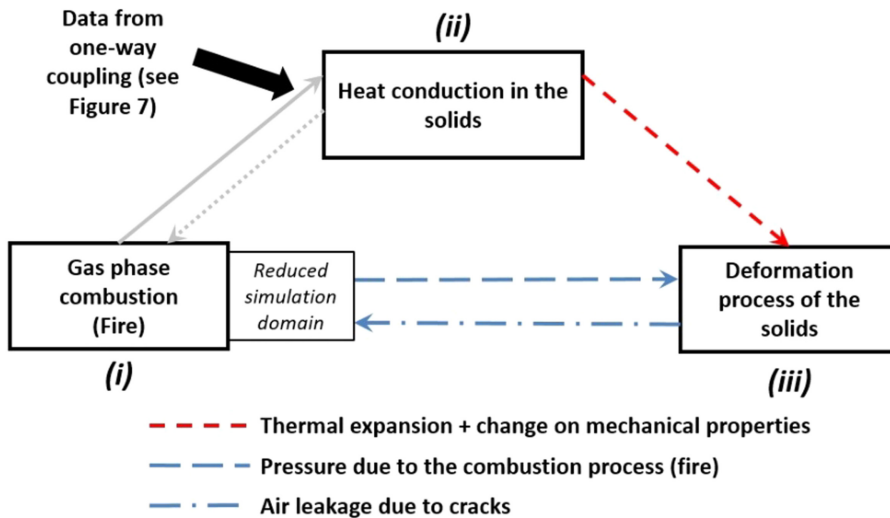
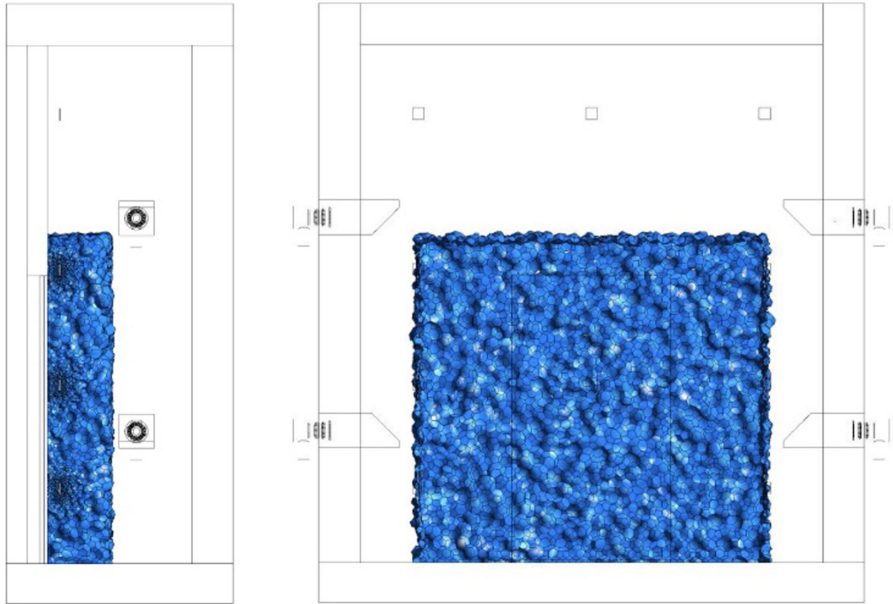


Figure 10. Methodology of the simplified two-way coupling approach

Source(s): Author's own creation



**Figure 11.**  
Geometry used in the one-way coupling approach and reduced domain for the STWC marked in blue

Source(s): Author's own creation

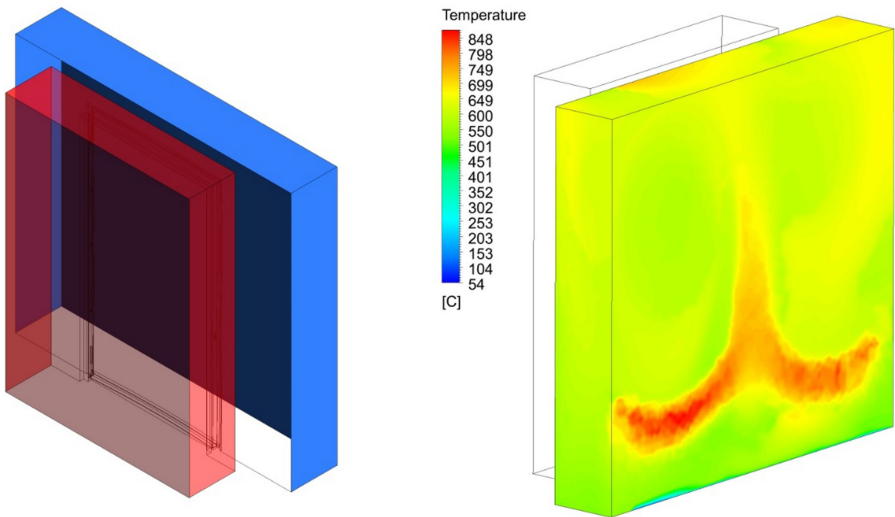


**Figure 12.**  
Reduced domain (gas phase in the furnace and gas phase ambient) (left); Temperature boundary at 360 s from the combustion simulation using one-way coupling (right)

Source(s): Author's own creation

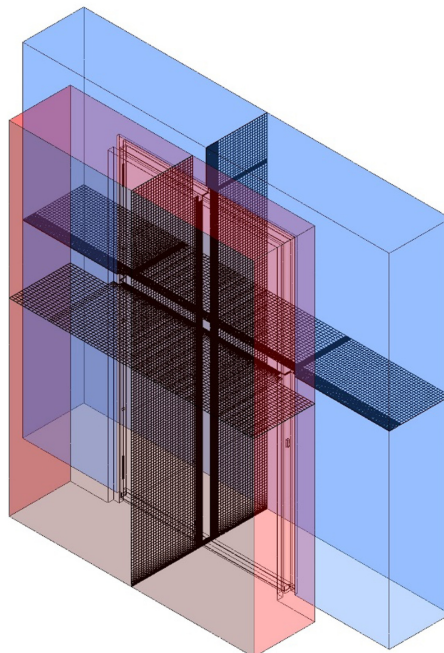
furnace (blue faces), the profiles for the temperature, pressure, velocity and radiation intensity extracted from the one-way coupling were used from each time step. For example, in [Figure 12](#) (right), the temperature profile at 360 s is highlighted. At the lower part, the effect of two burners can be identified by the hot zones. The flames of the lower burners were deflected

downwards by the baffle sheets, whereas the upper burner's flames were directed upwards with no visible effect at the boundary. The gas composition in the gas phase inside the furnace was chosen in accordance to the resulting gas from methane combustion with air with regard to a residual oxygen concentration of 6 vol%. This means that the gas has the same composition as calculated by the combustion model used for the one-way coupling.

It was found that for the simulation, a time step size of 2 s and a maximum number of two iterations between the CFD simulation of the gas phase and the FEM simulation of the deformation of the door were sufficient. The numerical grid for the domain (CFD) consists of approx. 1.5 million cells (hexahedrons), which can be seen in Figure 13. In the FEM simulation, the door frame represents the adjacent brick wall, which was assumed to be rigid. The numerical grid of the solid door and the adjacent frame consisted of approx. 77,000 cells (mainly hexahedrons). Dynamic meshing was applied to adapt the numerical grid according to the predicted deformation from the FEM simulation.

#### 4. Results and discussion

In this section, the results of both one-way coupling and STWC are discussed. The temperature and pressure inside the furnace will be presented in section 4.1, and the temperatures of the steel door (test specimen) are shown in section 4.2. In both sections, the results were calculated based on the one-way-coupling. The deformation of the steel door during the FRT will be considered in section 0, and a comparison between the one-way coupling and STWC will be presented. Eventually, the flue gas leakage predicted by the STWC approach will be highlighted in section 4.4.



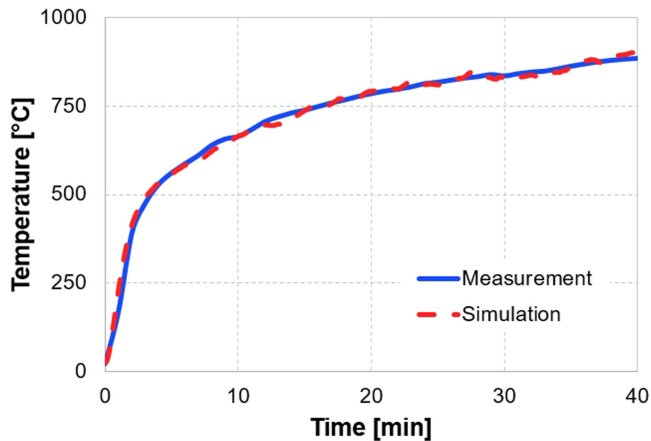
Source(s): Author's own creation

Figure 13.  
Numerical grid of the  
reduced domain for the  
gas phase

4.1 Temperatures and pressure in the fire resistance testing furnace

During the FRT, 12 plate thermocouples were arranged in a distance of 10 cm from the fire exposed surface of the door/wall. The average value of these thermocouples should represent the pre-defined temperature trend [see (European Committee for Standardization CEN, 2012)], which means that the thermal exposure of the door/wall is homogeneously distributed. The average temperature values are presented in Figure 14, where the blue line shows the measured temperature and the red line the predicted value. It can be seen that the predicted temperature during the entire testing time fits quite well with the experimental data.

Additionally, a volume rendering plot of the gas temperature in the furnace using the one-way coupling is presented after 10 min testing time in Figure 15 (left). Here, the deflection of the flames can be clearly seen and why the boundary profile for the STWC is highly affected by the lower burners. The boundary for the STWC is highlighted by the blue surface in this figure. In the furnace also a pressure gradient was detected, which can be clearly seen in Figure 15 (right). Two pressure measurement positions were arranged at the rear end of the furnace. The measurement position was about 50 cm below the ceiling, and the other one also



**Figure 14.** Measured and calculated temperature in the furnace

Source(s): Author's own creation

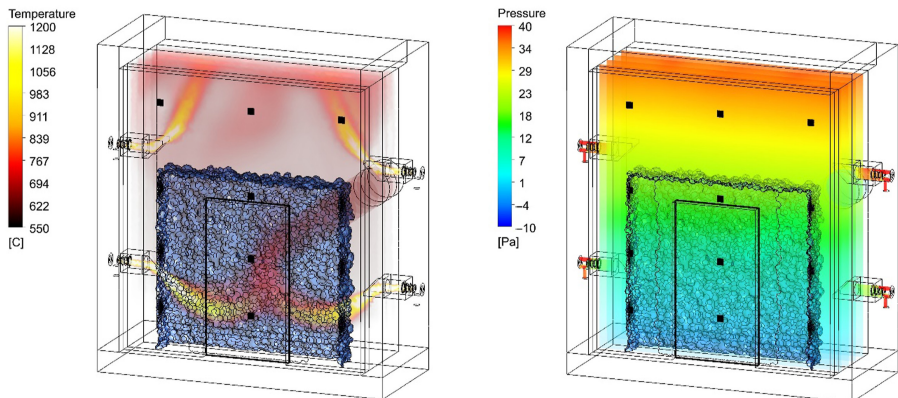


**Figure 15.** Volume rendering of the temperature (left) and the pressure (right) in the furnace after 10 min testing time

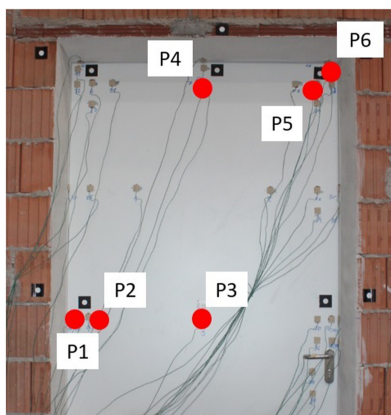
Source(s): Author's own creation

50 cm above the bottom of the furnace. The measurement showed that after the initial heating (approx. 5 min), the pressure in the furnace was constant. Therefore, the pressure shown in Figure 15 (right) is quite similar during the entire testing procedure. In the experiment, the measured pressure was 16 Pa (top) and 0.2 Pa (bottom). For comparison, the simulated pressure at the measurement positions showed values of 28 Pa and 0 Pa, which is slightly higher than the measured value. A reason for that is the missing flue gas leakage in the one-way coupling approach, which slightly decreases the pressure in the furnace.

Nevertheless, the pressure and temperature showed a good agreement with the experimental data and the profiles for the temperature, pressure, velocity and radiation intensity can be extracted and used in the STWC approach to predict the flue gas leakage and door deformation.

#### 4.2 Temperature of the steel door

In the one-way coupled approach also the temperature of the solid wall and test specimen was predicted in the CFD simulation (conjugate heat transfer). In Figure 16 (right), the calculated and measured temperatures at the steel door are presented after 40-min testing time. In addition, the measured and predicted temperatures during the entire testing time are presented in Figure 17. It can be seen that the highest temperatures were observed at “P1” and “P6”, which were located in a distance of 25 mm from the door’s corner/edge. At these positions, the temperature increased up to about 200°C. This can be explained by the faster heat transfer at the steel shell (thermal bridge) compared to the door’s centre, where gypsum and mineral wool represent a higher thermal resistance. The faster heat transfer at the corner/edge can be predicted by the numerical model in close accordance to the measurement. In a distance of 100 mm from the corner/edge (“P2”, “P4” and “P5”) and the door’s centre (“P3”), the temperature level was significantly lower in the experiment with a value of approx. 100°C. In general, the numerical simulation showed also similar values at “P2”, “P4” and “P5”. However, at the door’s centre, the predicted temperature was about 40 K lower. This is caused by the neglected water vapour inside the steel shell of the door, which is released from gypsum during the heating process. It was found by Prieler *et al.* (2020, 2022c) that the water vapour transport in the porous gypsum/mineral wool and the partial condensation/evaporation effects improve the heat transfer within porous structure. These effects were neglected, but a numerical methodology to take this into account can be found in Prieler *et al.* (2022c).



Source(s): Author’s own creation

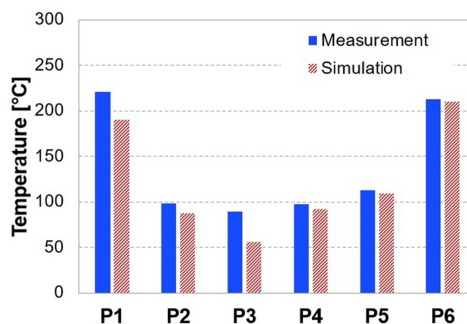


Figure 16. Measurement positions at the door (left) and measured/predicted temperatures at the door after 40-min testing time (right)

4.3 Deformation of the door

In Figure 18 the contour plot of the door’s deformation is presented. Here, only the plot of the STWC is shown because the one-way coupling’s plot is very similar and differences are barely visible. It can be seen that the door deforms to the fire unexposed side in the centre (marked by a positive value). In contrast, there is a large deformation to the fire exposed side at the upper and the bottom edge of the door. Also above the door lock, the door slightly deforms to the fire exposed side.

In accordance to the measurement positions, marked in Figures 2 and 18, the measured and predicted deformations are highlighted in Figure 19. Overall, similar results between the one-way and two-way coupling (STWC) approach can be detected. However, no flue gas leakage can be predicted by the one-way methodology. At the upper edge of the door (position “B”), the numerical models over-predicted the deformation with a value of about  $-30\text{ mm}$  (fire unexposed side), whereas the experiment showed a lower deformation. A reason for that is the missing deformation of the wall construction. The mechanical interaction between the door and the wall affects the deformation of both (wall and test specimen). This was investigated by Prieler *et al.* (2022b), where the wall deformation was also taken into account

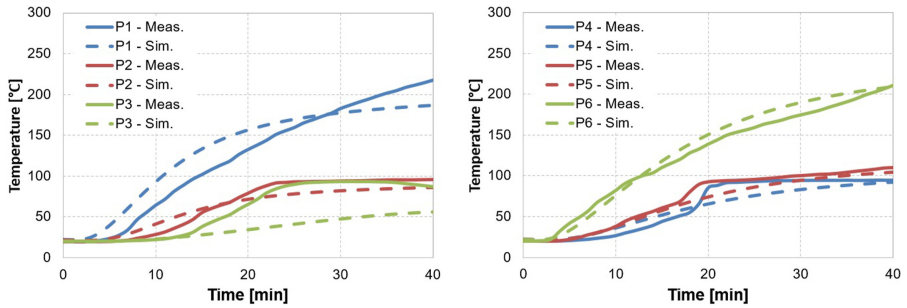


Figure 17. Measured and predicted temperatures at the door during the FRT

Source(s): Author’s own creation

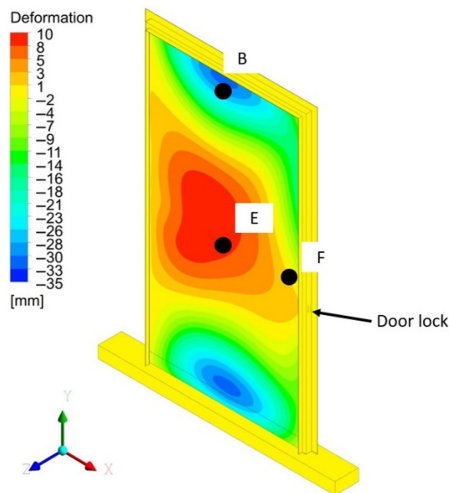


Figure 18. Contour plot of the door’s deformation in z-direction after 10 min using the STWC

Source(s): Author’s own creation

leading to a better agreement to the measurement at the upper edge. In contrast, the prediction of the deformation at the door's centre (position "E") was in close accordance to the measured value. After 10 min testing time the deformation was approx. 10 mm to the fire unexposed side (positive value). At position "F", which was located close to the door lock, the deformation was low.

Fire resistance  
test and  
prediction of  
leakage

#### 4.4 Gap modelling and flue gas leakage

The advantage of the STWC approach compared to the one-way coupling is the possibility to predict the gap formation as well as the flue gas leakage from the furnace. Flue gas leakage from the furnace is possible due to (1) mechanical failure of components [e.g. (Feenstra *et al.*, 2018; de Boer *et al.*, 2019)] or (2) gap formation between the solids. In the present study, the focus was on the gap formation between the door and the wall, which is highlighted in Figure 20. In this figure, two main gaps can be identified. One gap was at the upper edge of the door, and the second one was located on the right hand side of the door (above the door lock).

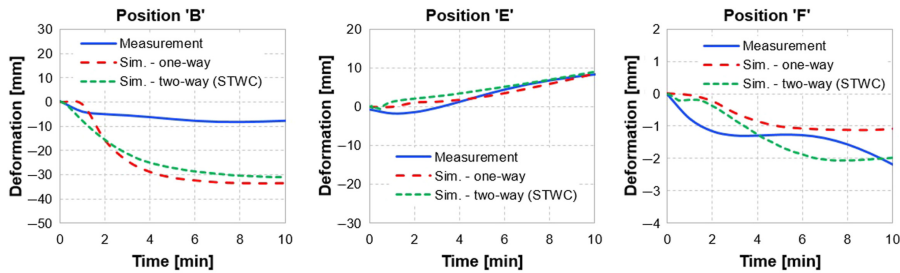


**Figure 19.** Measured and simulated deformation of the steel door at position "B", "E" and "F"

Source(s): Author's own creation

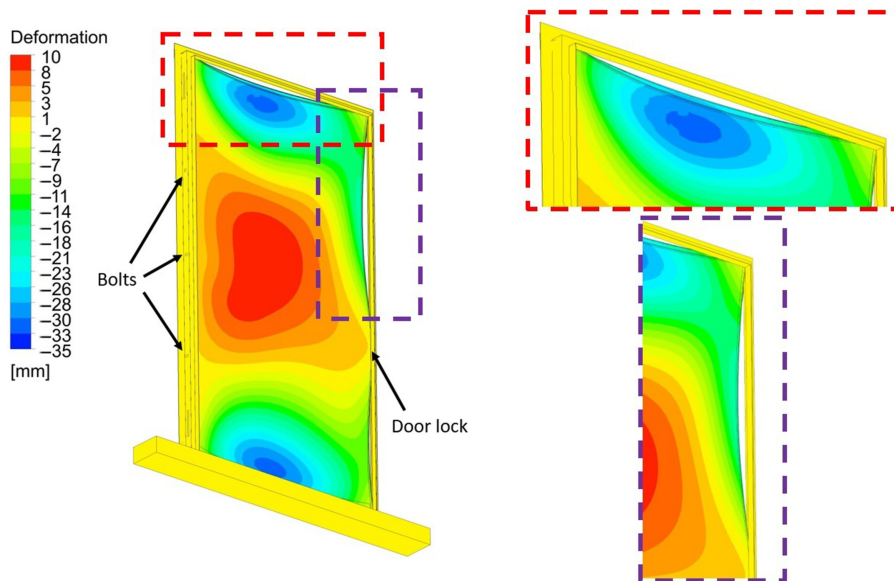


**Figure 20.** Predicted gap formation between the door and the door's frame/wall by the STWC after 10 min testing time (deformation scale: 4x)

Source(s): Author's own creation

To compare the position of the gaps with the FRT, [Figure 21](#) (left) shows the door with a clearly visible gap at the upper edge. The gap above the door lock can be hardly identified on pictures, however the damages above the door lock clearly shows the contact with the flue gas from inside the furnace (see red mark in [Figure 21](#) (right)). It has to be mentioned that also on the left hand side of the door flue gas leakage was determined, however, the gap formation and flue gas leakage from the furnace were at a low level due to the bolts located at this side of the door. It can be concluded that the position of the gap formation can be predicted by the numerical model in close accordance to the experimental observations.

The simulated flue gas leakage from the gaps at the door's upper edge and above the door lock is shown in [Figure 22](#). In the side view, it is visible that the majority of the leakage occurs at the door's upper edge, although the exact position there cannot be identified from this figure. In the front view, there is also a slight flue gas leakage visible above the door lock (coming from the right hand side). This flue gas leakage is directed to the centre of the door and sums up with the flue gas



**Figure 21.** Observed gap formation during the fire resistance test at the upper edge of the door (left) and burning marks above the door lock after the test (right)

Source(s): Author's own creation

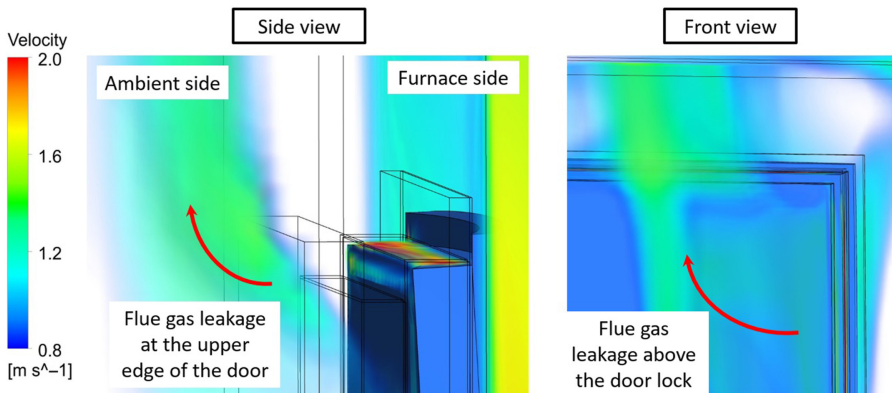


**Figure 22.** Predicted flue gas leakage at the upper edge of the door (left) and above the door lock (right)

Source(s): Author's own creation

leakage from the door's upper edge. Since the flue gas leakage at the left hand side of the door is much lower, due to the smaller gaps (bolts), the same effect was not observed from the left hand side and the flue gas flow-rate is lower on this side. This can be also observed during the FRT. In Figure 23 (top), the condensed water marks at the concrete lintel at the door's upper edge are shown. In Figure 23 also a scale was inserted, which extends from the left hand side of the door to the right hand side. Due to the cooler surface of the lintel, the water vapour in the flue gas from the furnace condenses there. Therefore, the size of the water mark is a measure for the amount of flue gas flow at this position. During the FRT, two main regions of water marks were observed. A smaller region was determined between 22 and 42% of the door's width (see red mark) and a larger region was located between 50 and 85% (orange mark). The larger region is an indication for the additional flue gas leakage above the door lock, which sums up with the leaked flue gas from the door's upper edge. Due to the smaller gaps on the left hand side of the door, the region of the water mark is smaller. The STWC approach used in this study was not only capable to determine the position of the gap formation, but also the amount of flue gas exiting the furnace, which can be seen in Figure 23 (bottom). The position of the flue gas hitting the concrete lintel is similar to the observed water marks in the experiment. The simulation showed that the flue gas was between 20 and 40% as well as 50 and 80%.

## 5. Conclusion

In the present study, a STWC methodology was introduced to predict the fluid flow of the combustion flue gases, the heat transfer in the solid test specimen and its deformation as well as the gap formation and flue gas leakage. For this purpose, a FRT of a steel door, embedded in a brick wall, was carried out to obtain the validation data. Two-way coupling methodologies are

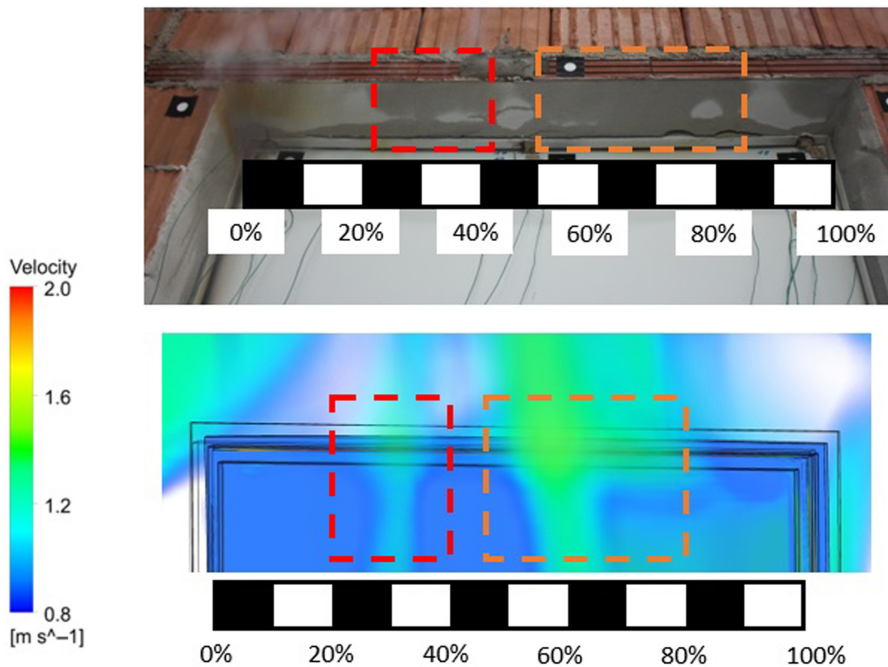


**Figure 23.**  
Condensed water  
marks at the door's  
upper edge (top) and  
position of the  
predicted flue gas  
leakage (bottom)

Source(s): Author's own creation

---

still rare in fire science. Despite some two-way approaches, which consider the mechanical failure of solid components, there is no study available at the moment considering the two-way coupling where flue gas leakage caused by the gap formation occurs. Thus, the present study tried to address this issue with the proposed STWC with the following findings:

- (1) The calculated temperatures inside the furnace and at the solid test specimen (steel door) were found to be in good agreement with the measured data. However, the temperature at the door's centre was about 40 K lower due to the missing water vapour transport model and neglected condensation/evaporation effects inside the door.
- (2) At the door's centre, the deformation of the door was about 10 mm to the fire unexposed side, which was also calculated by the numerical STWC methodology.
- (3) The STWC determined the main gap formation between the steel door and the wall at the door's upper edge as well as the right hand side of the door (above the door lock). Only a minor gap formation was found at the door's left hand side. These findings were determined by the observed gap formation in the experiment.
- (4) Besides the correct prediction of the gaps, also the flow-rate/amount of flue gas was well predicted and fits quite well with the water marks at the concrete lintel above the door, where water from the flue gas condenses.

It can be concluded that the STWC was capable to predict the deformation, gap formation and flue gas leakage during FRTs. Further studies will include also the combustion process in the furnace and water vapour transport inside the steel door to improve the numerical predictions.

## References

- Alos-Moya, J., Paya-Zaforteza, I., Garlock, M.E.M., Loma-Ossorio, E., Schiffner, D. and Hospitaler, A. (2014), "Analysis of a bridge failure due to fire using computational fluid dynamics and finite element models", *Engineering Structures*, Vol. 68, pp. 96-110.
- ANSYS (2013), *ANSYS Fluent Theory Guide 15.0, 2013*, ANSYS Incorporate, Canonsburg, PA.
- ANSYS (2020a), *ANSYS Mechanical User's Guide Release 2020 R2*, ANSYS Incorporate, Canonsburg, PA.
- ANSYS (2020b), *Fluent Theory Guide Release 2020 R2*, ANSYS Incorporate, Canonsburg, PA.
- BS EN1993-1-2 (1993), "Eurocode 3: design of steel structures – part 1-2: general rules – structural fire design".
- Cabova, K., Liskova, N., Benysek, M., Zeman, F. and Wald, F. (2017), *Numerical Simulation of Fire-Resistance Test of Steel Beam*, pp. 2518-2525, EUROSTEEL, Copenhagen, Denmark.
- Chui, E. and Raithby, G. (1993), "Computation of radiant heat transfer on a nonorthogonal mesh using the finite-volume method", *Numerical Heat Transfer, Part B: Fundamentals*, Vol. 23, pp. 269-288.
- de Boer, J.G.G.M., Hofmeyer, H., Maljaars, J. and van Herpen, R.A.P. (2019), "Two-way coupled CFD fire and thermomechanical FE analyses of a self-supporting sandwich panel façade system", *Fire Safety Journal*, Vol. 105, pp. 154-168.
- Duthinh, D., McGrattan, K. and Khaskia, A. (2008), "Recent advances in fire-structure analysis", *Fire Safety Journal*, Vol. 43 No. 2, pp. 161-167.
- European Committee for Standardization CEN (2012), *European Standard EN 1363-1, Fire Resistance Test-Part 1: General Requirements*, Brussels.
- Feenstra, J.A., Hofmeyer, H., Van Herpen, R.A.P. and Mahendran, M. (2018), "Automated two-way coupling of CFD fire simulations to thermomechanical FE analyses at the overall structural level", *Fire Safety Journal*, Vol. 96, pp. 165-175.

- 
- JMatPro (2005), *User's Guide*, Sente Software Limited, Guildford.
- Lazaro, D., Puente, E., Lazaro, M., Lazaro, P.G. and Pena, J. (2016), "Thermal modelling of gypsum plasterboard assemblies exposed to standard fire tests", *Fire Mater*, Vol. 40, pp. 568-585.
- Luecke, W., Banovic, S.W. and McColskey, J.D. (2011), "NIST technical note 1714—high-temperature tensile constitutive data and models for structural steels in fire".
- Malendowski, M. and Glema, A. (2017), "Development and implementation of coupling method for CFD-FEM analyses of steel structures in natural fire", *Procedia Engineering*, Vol. 172, pp. 692-700.
- McGrattan, K., McDermott, R., Weinschenk, C. and Forney, G. (2013), "Fire dynamics simulator, technical reference Guide, sixth edition, special publication (NIST SP)–1019".
- Peters, N. (1984), "Laminar diffusion flamelet models in non-premixed turbulent combustion", *Progress in Energy and Combustion Science*, Vol. 10 No. 3, pp. 319-339.
- Peters, N. (1988), "Laminar flamelet concepts in turbulent combustion", *21st Symposium on Combustion*, The Combustion Institute. pp. 1231-1250.
- Prasad, K. and Baum, H.R. (2005), "Coupled fire dynamics and thermal response of complex building structures", *Proceedings of the Combustion Institute*, Vol. 30 No. 2, pp. 2255-2262.
- Prieler, R., Mayr, B., Demuth, M., Holleis, B. and Hochenauer, C. (2016), "Prediction of the heating characteristic of billets in a walking hearth type reheating furnace using CFD", *International Journal of Heat and Mass Transfer*, Vol. 92, pp. 675-688.
- Prieler, R., Mayrhofer, M., Eichhorn-Gruber, M., Schwabegger, G. and Hochenauer, C. (2018a), "A numerical methodology to predict the gas/solid interaction in fire resistance tests", *10th International Conference on Structures in Fire*, Belfast, pp. 383-390.
- Prieler, R., Mayrhofer, M., Gaber, C., Gerhardtter, H., Schluckner, C., Landfahner, M., Eichhorn-Gruber, M., Schwabegger, G. and Hochenauer, C. (2018b), "CFD-based optimization of a transient heating process in a natural gas fired furnace using neural networks and genetic algorithms", *Applied Thermal Engineering*, Vol. 138, pp. 217-234.
- Prieler, R., Mayrhofer, M., Eichhorn-Gruber, M., Schwabegger, G. and Hochenauer, C. (2019a), "Development of a numerical approach based on coupled CFD/FEM analysis for virtual fire resistance tests—part A: thermal analysis of the gas phase combustion and different test specimens", *Fire Mater*, Vol. 43 No. 1, pp. 34-50.
- Prieler, R., Gerhardtter, H., Landfahner, M., Gaber, C., Schluckner, C., Eichhorn-Gruber, M., Schwabegger, G. and Hochenauer, C. (2019b), "Development of a numerically efficient approach based on coupled CFD/FEM analysis for virtual fire resistance tests— part B: deformation process of a steel structure", *Fire Mater*, Vol. 44, pp. 704-723.
- Prieler, R., Kitzmüller, P., Thumser, S., Schwabegger, G., Kaschnitz, E. and Hochenauer, C. (2020), "Experimental analysis of moisture transfer and phase change in porous insulation exposed to fire and its effect on heat transfer", *International Journal of Heat and Mass Transfer*, Vol. 160, 120207.
- Prieler, R., Kitzmüller, P., Thumser, S., Schwabegger, G. and Hochenauer, C. (2023), "Experimental analysis of the wall deformation of masonry brick and gypsum-sheathed stud walls during standardized fire resistance tests of steel doors", *Fire Mater*, Vol. 47, pp. 305-321.
- Prieler, R., Klemm, B., Pletzer, S., Thumser, S., Schwabegger, G. and Hochenauer, C. (2021), "Pressure increase in enclosures of steel doors and its effect on the deformation process during fire resistance tests – a numerical study", *Proceedings Applications of Structural Fire Engineering*, pp. 174-179.
- Prieler, R., Ortner, B., Kitzmüller, P., Thumser, S., Schwabegger, G. and Hochenauer, C. (2022a), "Numerical analysis of the masonry brick wall's deformation with embedded steel door during a fire resistance test", *12th International Conference on Structures in Fire*, Hong Kong, China, pp. 648-659.
- Prieler, R., Langbauer, R., Gerhardtter, H., Kitzmüller, P., Thumser, S., Schwabegger, G. and Hochenauer, C. (2022b), "Modelling approach to predict the fire-related heat transfer in porous gypsum based on multi-phase simulations including water vapour transport, phase change and radiative heat transfer", *Applied Thermal Engineering*, Vol. 206, 118013.

- 
- Raithby, G.D. and Chui, E.H. (1990), "A finite-volume method for predicting a radiant heat transfer in enclosures with participating media", *Journal of Heat Transfer*, Vol. 112, pp. 415-423.
- Richter, F. (n.d.), "The physical properties of steels "the 100 steels programme" part I: tables and figures", available at: [https://www.tugraz.at/fileadmin/user\\_upload/Institute/IEP/Thermophysics\\_Group/Files/Staehle-Richter.pdf](https://www.tugraz.at/fileadmin/user_upload/Institute/IEP/Thermophysics_Group/Files/Staehle-Richter.pdf)
- Sandström, J., Wickström, U. and Veljkovic, M. (2009), "Adiabatic surface temperature—a sufficient input data for a thermal model", *Application of Structural Fire Engineering*, Prague, Czech Republic, pp. 1-7.
- Shih, T.-H., Liou, W.W., Shabbir, A., Yang, Z. and Zhu, J. (1995), "A new  $k-\epsilon$  eddy viscosity model for high reynolds number turbulent flows", *Computers Fluids*, Vol. 24 No. 3, pp. 227-238.
- Silva, J.C.G., Landesmann, A. and Ribeiro, F.L.B. (2014), "Performance-based analysis of cylindrical steel containment Vessels exposed to fire", *Fire Safety Journal*, Vol. 69, pp. 126-135.
- Silva, J.C.G., Landesmann, A. and Ribeiro, F.L.B. (2016), "Fire-thermomechanical interface model for performance-based analysis of structures exposed to fire", *Fire Safety Journal*, Vol. 83, pp. 66-78.
- Smith, T.F., Shen, Z.F. and Friedman, J.N. (1982), "Evaluation of coefficients for the weighted sum of gray gases model", *Journal of Heat Transfer*, Vol. 104 No. 4, 602.
- Szymkuć, W., Glema, A., Malendowski, M., Mielcarek, A., Smardz, P. and Poteralski, A. (2018), "Numerical investigation of fire and post-fire performance of CFT columns in an open car park", *Proceedings of the 10th International Conference on Structures in Fire*, Belfast, pp. 407-414.
- Tondini, N., Vassart, O. and Franssen, J. (2012), "Development of an interface between CFD and FE software", *7th International Conference on Structures in Fire*, Zurich, Switzerland, pp. 459-468.
- Welch, S., Miles, S., Kumar, S., Lemaire, T. and Chan, A. (2008), "FIRESTRUC—integrating advanced three-dimensional modelling methodologies for predicting thermo-mechanical behaviour of steel and composite structures subjected to natural fires", *Fire Safety Science*, Reykjavik, Iceland, pp. 1315-1326.
- Wickström, U. (2016), "Methods for predicting temperatures in fire-exposed structures", *SFPE Handbook of Fire Protection Engineering*, Springer-Verlag, NY.
- Wickström, U., Duthinh, D. and McGrattan, K. (2007), "Adiabatic surface temperature for calculating heat transfer to fire exposed structures", *Interflam 2007 11th International Interflam Conference*, London, UK.
- Wickström, U., Robbins, A. and Baker, G. (2011), "The use of adiabatic surface temperature to design structures for fire exposure", *Journal of Structural Fire Engineering*, Vol. 2 No. 1, pp. 21-28.
- Yu, X. and Jeffers, A.E. (2013), "A comparison of subcycling algorithms for bridging disparities in temporal scale between the fire and solid domains", *Fire Safety Journal*, Vol. 59, pp. 55-61.
- Zhang, C., Silva, J.G., Weinschenk, C., Kamikawa, D. and Hasemi, Y. (2016), "Simulation methodology for coupled fire-structure analysis: modeling localized fire tests on a steel column", *Fire Technology*, Vol. 52 No. 1, pp. 239-262.

### Corresponding author

Rene Prieler can be contacted at: [rene.prieler@tugraz.at](mailto:rene.prieler@tugraz.at)

---

For instructions on how to order reprints of this article, please visit our website:

[www.emeraldgroupublishing.com/licensing/reprints.htm](http://www.emeraldgroupublishing.com/licensing/reprints.htm)

Or contact us for further details: [permissions@emeraldinsight.com](mailto:permissions@emeraldinsight.com)